Magnetodielectric properties of spin-orbital coupled system Mn₃O₄

Takehito Suzuki[1] and Takuro Katsufuji[1,2,3]

[1]*Department of Physics, Waseda University, Tokyo 169-8555, Japan*
[2]*Kagami Memorial Laboratory for Material Science and Technology, Waseda University, Tokyo 169-0051, Japan*
[3]*PRESTO, Japan Science and Technology Agency, Saitama 332-0012, Japan*

We studied the dielectric properties and strain of spinel Mn_3O_4 with applied magnetic field. It was found that the dielectric constant (ε_1) exhibits a large magnetic-field (H) dependence, which is anisotropic both against the direction of the magnetic field and the electric field in the magnetically ordered phases below $T_N = 43$ K. It was also found that the $\varepsilon_1(H)$ exhibits distinctively different behaviors at three different magnetic phases. These results can be explained by the change of the orbital state of Mn^{3+} with the applied magnetic field due to the inverse process of single-ion spin anisotropy.

Ferrimagnetic spinel oxides with two transition metals often exhibit an intriguing magnetic-field effect on their dielectric and structural properties. One example is $CoCr_2O_4$ showing a multiferroic behavior.[1] In this compound, ferroelectric polarization appears simultaneously with the magnetic ordering of a cycloidal spin structure, and this ferroelectricity is caused by the so-called inverse Dzyaloshinskii-Moriya mechanism, i.e., noncollinear spins at the neighboring sites shift the anion in between.[2,3] A unique magnetic-field effect in this compound is that the direction of the ferroelectric polarization can be switched by applied different directions of magnetic field.

Another example of the magnetic-field effect on the dielectric and structural properties is seen in spinel vanadates, MnV_2O_4 and FeV_2O_4,[4,5] showing orbital ordering. In these compounds, the orbital degree of freedom in the V^{3+} ion, in which two electrons occupy the triply degenerate t_{2g} orbitals, exhibits antiferroic ordering simultaneously with ferrimagnetic ordering (57 K for MnV_2O_4), and this orbital ordering is caused by the so-called Kugel-Khomskii interaction, i.e., interionic spin-orbit coupling.[6,7] These compounds exhibit a large magnetostriction and magnetocapacitance due to the alignment of the crystalline domains by applied magnetic field, another type of magnetic-field effect in ferrimagnetic spinel oxides.

Recently, polycrystalline Mn_3O_4 has been found to show magnetocapacitance around Néel temperature $T_N = 43$ K and at lower temperatures.[8,9] This compound has Mn^{2+} ions ($3d^5$) at the tetrahedral site and Mn^{3+} ions ($3d^4$) at the octahedral site of the spinel structure [Fig. 1(a)], and is tetragonally distorted (space group is $I4_1/amd$) below $T_s = 1443$ K to lift the orbital degeneracy of the Mn^{3+} ion, where there is one electron in the doubly degenerate e_g orbital.[10] This compound exhibits a magnetic transition from a paramagnetic to a Yafet–Kittel phase at $T_N = 43$ K.[11–13] In this Yafet-Kittel phase, the Mn^{2+} spin at the tetrahedral site is aligned along the [110] direction in the cubic settings, and the sum of the Mn^{3+} spins at the octahedral site is antiparallel to the Mn^{2+} spin, but each spin is canted from the [−1−10] direction toward the [001] or [00−1] direction [Fig. 1(b)]. This compound has further magnetic transitions at $T_1 = 39$ K and $T_2 = 33$ K.[11] Between T_2 and T_1, the magnetic unit cell becomes incommensurate with respect to the chemical unit cell ("in-

commensurate" phase). Below $T_2 = 33$ K, the magnetic unit cell becomes commensurate with the chemical unit cell again, but is doubled along the [110] direction compared to the Yafet-Kittel phase ("cell-doubled" phase).

Since both the crystal structure and the magnetic structures are anisotropic in Mn_3O_4, it is necessary to study single crystals to understand its magnetodielectric properties. In this Rapid Communication, we report the measurement of the dielectric constant and strain in Mn_3O_4 single crystals with applied magnetic field. We found that the dielectric constant of this compound exhibits a peculiar magnetic-field dependence at each magnetic phase, which is caused by the change of the e_g orbital state in the Mn^{3+} ion with applied magnetic field.

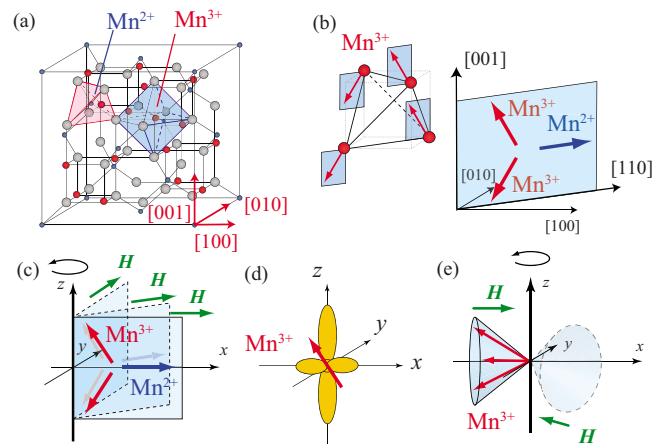Single crystals of Mn_3O_4 were grown by a floating zone

FIG. 1. (Color online) (a) Schematic picture of the spinel structure. The $\langle 100 \rangle$ axis is taken parallel to the direction of the Mn-O bond of the MnO_6 octahedron. (b) The magnetic structure of the Yafet-Kittel phase ($T_1 < T < T_N$). The Mn^{2+} and the Mn^{3+} spins lie on the (1–10) plane. (c) Schematic image of the rotation of the spin with applied H in the coplanar magnetic structure phase (the Yafet-Kittel and the cell-doubled phase). (d) Illustration of the orbital state of Mn^{3+} with the spin state shown in (c). (e) Schematic picture of the conical Mn^{3+} spins with the [110] cone axis and the rotation of the cone with applied H in the incommensurate phase ($T_2 < T < T_1$).
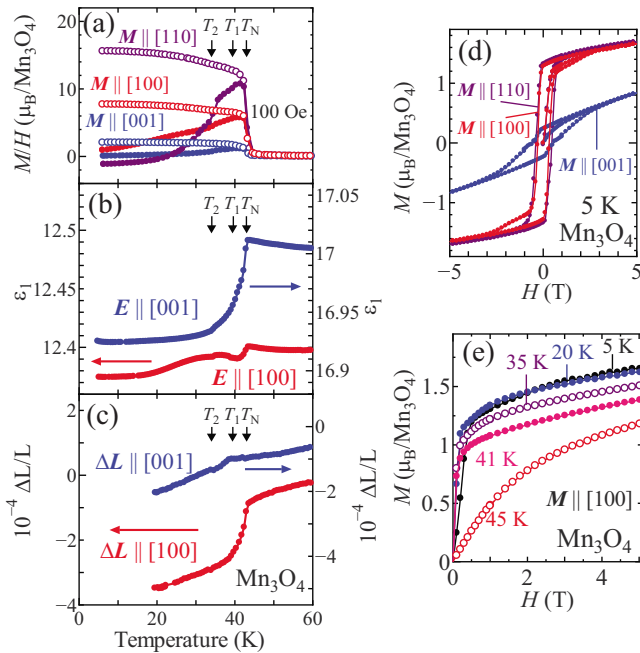
FIG. 2. (Color online) (a) Temperature dependence of magnetization with applied 100 Oe. The open (closed) circles denote the magnetization in the field-cooling (zero-field-cooling) procedure. Temperature dependence of (b) dielectric constant and (c) strain along the $[100]$ direction (in-plane, left axis) and the $[001]$ direction (out-of-plane, right axis) without applied magnetic field. (d) Magnetic-field dependence of magnetization along the $[100]$, $[110]$ (in-plane) and $[001]$ (out-of-plane) direction at 5 K. (e) Magnetic-field dependence of magnetization along the $[100]$ direction at various temperatures.

method. The crystals were oriented by the x-ray back Laue reflection technique and cut into a disk shape along the (100) or (001) plane. In this Rapid Communication, we take the hkl indices in which the $[100]$ direction is along the Mn-O bond of the MnO_6 octahedron perpendicular to the c axis [Fig. 1(a)]. We measured the dielectric constant using a capacitance bridge at 1 kHz with an applied magnetic field up to 5 T. Silver paste was painted as electrodes. Strain measurement was performed by a conventional strain-gauge technique. Magnetization was measured by the superconducting quantum interference device (SQUID) magnetometer. Spontaneous polarization was also searched by pyroelectric current measurement, but was found to be zero within the experimental error ($P < 1$ $\mu C/m^2$).

Figure 2(a) shows the temperature (T) dependence of magnetization (M) at 100 Oe in Mn_3O_4. M sharply increases at $T_N = 43$ K, which is the onset of the Yafet-Kittel phase. The magnetic-field (H) dependence of M in three different directions is shown in Fig. 2(d). The magnitude of M is substantially smaller along the $[001]$ direction, indicating that the c axis is the magnetically hard axis in this compound. The difference between $M \| [100]$ and $M \| [110]$ is not clearly observed in Fig. 2(d), but is observed in the $M(T)$ curve measured at 100 Oe shown Fig. 2(a). This means that, though there exists in-plane magnetic anisotropy with the easy axis along the $[110]$ direction, it is much smaller than the anisotropy between parallel and perpendicular to the ab

plane [(001) plane]. Figure 2(e) shows the H dependence of M along the $[100]$ direction at several temperatures. In all the magnetically ordered phases ($T < T_N = 43$ K), M increases steeply in the low H region.

The T dependence of the in-plane and out-of-plane dielectric constant (ε_1) is shown in Fig. 2(b). Both ε_1 with $E \| [100]$ (in-plane) and with $E \| [001]$ (out-of-plane) decrease steeply at T_N, but the amount of the decrease is larger for the out-of-plane dielectric constant ($\Delta \varepsilon_1 / \varepsilon_1 \sim 4 \times 10^{-3}$) than for the in-plane dielectric constant ($\Delta \varepsilon_1 / \varepsilon_1 \sim 1 \times 10^{-3}$). Smaller anomalies are also observed both at $T_1 = 39$ K, which is the magnetic transition temperature from the Yafet-Kittel to incommensurate phase, and $T_2 = 33$ K, from the incommensurate to the cell-doubled phase. The dielectric loss was barely observed in this T range (not shown). These anomalies of ε_1 at the magnetic transition temperatures indicate the correlation between the dielectric and magnetic properties in this compound.

The temperature dependence of strain ($\Delta L / L$) also exhibits anomalies at the magnetic transition temperatures [Fig. 2(c)], indicating the correlation also between structural and magnetic properties. However, the magnitude of $\Delta L / L$ at T_N ($\Delta L / L \sim 2 \times 10^{-4}$) is much smaller than that of $\Delta \varepsilon_1 / \varepsilon_1$. These results exclude the possibility that only the strain of the crystal is the origin of the decrease in capacitance at T_N shown in Fig. 2(b).

This compound exhibits a large response of both dielectric constant and strain against magnetic field. Figure 3(a) shows the T dependence of the in-plane ε_1 ($E \| [100]$) with applied H. When in-plane H is applied parallel to the direction of the electric field (E), in-plane ε_1 is suppressed below T_N (closed circles). On the other hand, when in-plane H is applied perpendicular to E, the in-plane ε_1 is enhanced (open circles). In both cases, the magnitude of magnetocapacitance $[\varepsilon_1(H)/\varepsilon_1(0) - 1]$ amounts to $\sim 2\%$ at 5 T. However, when out-of-plane H (along the $[001]$ axis) is applied, the in-plane ε_1 barely changes (open squares). The in-plane strain ($\Delta L / L$ along the $[100]$) shows a similar anisotropy, namely, the crystal is elongated along the direction of H but contracted perpendicular to H in the ab plane below T_N [Fig. 3(b)]. This kind of anisotropic magnetic-field dependence of dielectric constant and strain resembles that of MnV_2O_4, FeV_2O_4, and $Tb_3Fe_5O_{12}$,[4,5,14] where the tetragonal or orthorhombic domains can be aligned with applied magnetic field.

The T dependences of the out-of-plane ε_1 ($E \| [001]$) with applied H of 5 T is shown in Fig. 3(c). The behavior is quite different from that of the in-plane ε_1; the out-of-plane ε_1 is suppressed with applied H (negative magnetocapacitance) for both in-plane and out-of-plane magnetic field H only around T_N. This behavior of magnetocapacitance along the c axis is quite similar to those observed in $EuTiO_3$ (Ref. 15) and $BiMnO_3$,[16] or to that of magnetoresistance observed in perovskite manganites. The magnitude of the suppression is larger for the in-plane H presumably due to the larger in-plane magnetization shown in Fig. 2(a). It should be noted that the magnetocapacitance observed in polycrystalline samples[8,9] can be regarded as the sum of the in-plane and out-of-plane magnetocapacitance of the single crystal.

To see the coupling between magnetic and dielectric properties in more detail, magnetic-field dependence of the in-
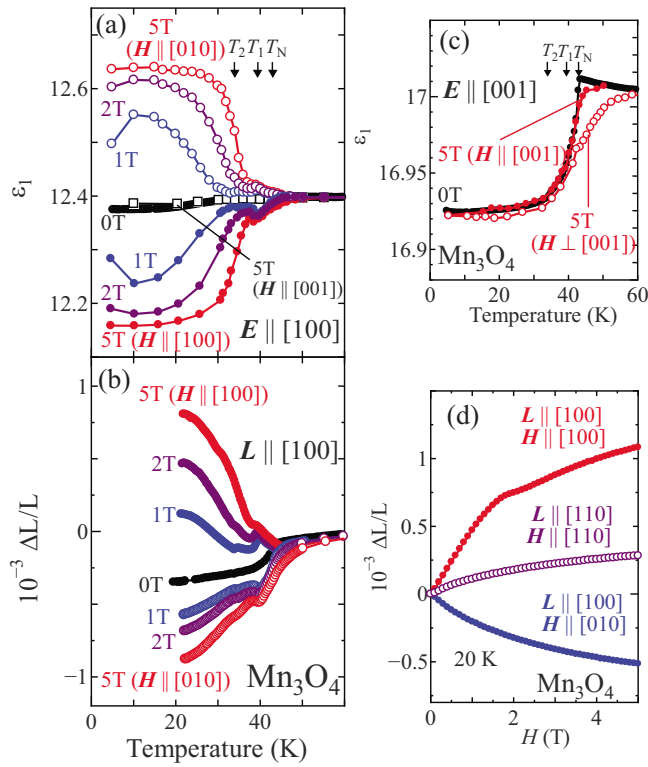
FIG. 3. (Color online) Temperature dependence of (a) the dielectric constant and (b) strain along the [100] direction with applied magnetic field. (c) Temperature dependence of the dielectric constant along the [001] direction (out-of-plane). (d) Magnetic-field dependence of the in-plane strain at 20 K. The closed circles denote the strain along the [100] direction and the open ones denote that along the [110] direction.

plane dielectric constant with in-plane $H \perp E$ is shown in Figs. 4(a) and 4(b). For $T_1 = 39$ K $< T < T_N = 43$ K (in the Yafet-Kittel phase, closed circles), a steep increase in the in-plane dielectric constant in the low H region (<0.2 T) is
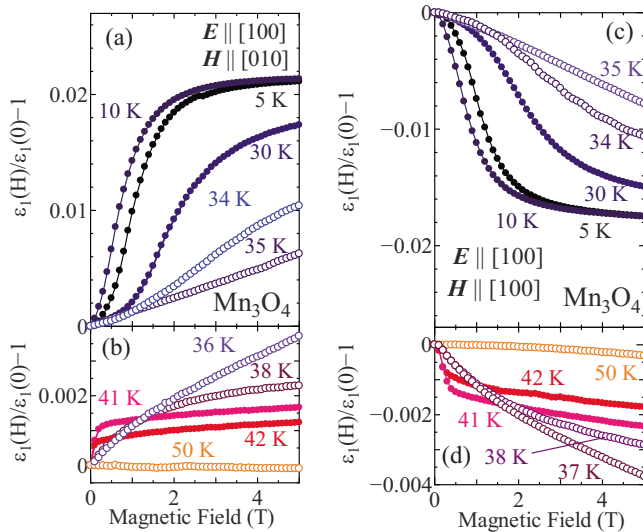

FIG. 4. (Color online) Magnetic-field dependence of the dielectric constant along the [100] direction with [(a) and (b)] $H \perp E$ and [(c) and (d)] $H \| E$.

followed by an almost flat H dependence in the higher H region. For $T_2 = 33$ K $< T < T_1 = 39$ K (in the incommensurate phase, open circles), the sharp increase in the dielectric constant in the low H region disappears, but only a gradual increase up to 5 T is observed. Below $T_2 = 33$ K (in the cell doubled phase, closed circles), a fairly steep increase in dielectric constant in the low H region appears again. We also measured the H dependence of the in-plane dielectric constant with $H \| E$ [Figs. 4(c) and 4(d)], and found that the behaviors are quite similar to those with $H \perp E$ shown in Figs. 4(a) and 4(b), except for the difference of the sign. These results indicate that, though the H dependence of M exhibits a sharp increase in the low H region at all magnetic phases, as shown in Fig. 2(e), ε_1 exhibits a peculiar H dependence at each magnetic phase.

The dielectric constant at 1 kHz is primarily dominated by optical phonons, and so, magnetocapacitance is caused by the change of the optical-phonon frequency and/or the effective charge of the ions with magnetic field. Since the magnetocapacitance of Mn_3O_4 is anisotropic, it is likely that the variation of the force constants between the ions with the applied magnetic field leads to the variation of phonon frequencies and the resulting magnetocapacitance. Below, we mainly discuss the mechanism of the in-plane magnetocapacitance in this compound.

In the Yafet-Kittel phase ($T_1 = 39$ K $< T < T_N = 43$ K), a Mn^{2+} spin and two Mn^{3+} spins are aligned in a "triangular" structure, where these three spins lie on the same (1–10) plane (coplanar spin structure) in the ground state, and the net magnetic moment is along the [110] direction, as shown in Fig. 1(b). However, this plane can be easily rotated around the [001] axis with the applied magnetic field [Fig. 1(c)], based on the small in-plane anisotropy of magnetization. Accordingly, if the magnetic field is applied along the [100] direction, the Mn^{2+} and Mn^{3+} spins lie on the (010) plane, and the Mn^{3+} spins are pointed to a direction between the [001] (or [00−1]) and the [−100] direction.

On the basis of this spin structure, let us discuss the Mn^{3+} orbital state in this phase. Since the c axis is elongated in the tetragonal phase of Mn_3O_4,[10] the e_g state of Mn^{3+} is split into the z^2 state with lower energy and the x^2-y^2 state with higher energy, and thus the z^2 state is occupied by an electron. Because of the single-ion spin anisotropy, which arises from the second-order perturbation of spin-orbit coupling for the e_g state,[17] the Mn^{3+} spin prefers to be oriented along the c axis. In reality, the Mn^{3+} spin is canted toward the [−100] direction when magnetic-field is applied along the [100] direction. This canting of the Mn^{3+} spin induces the hybridization of the x^2 state (or equivalently, z^2-x^2 state) to the z^2 state as the orbital state of the spin through the inverse process of single-ion spin anisotropy, as shown in Fig. 1(d). This hybridization leads to the anisotropy of the force constant of the $Mn^{3+}-O^{2-}$ bond in the x direction and the y direction, and this change of the force constants causes the change of the phonon frequencies and the resulting magnetocapacitance. In this mechanism, the H dependence of the dielectric constant should scale with the H dependence of magnetization, consistent with the experimental result that both values exhibit a sharp increase in the low H region. This can also explain the smaller response of strain when mag-

netic field is applied along the [110] direction, as shown in Fig. 3(d), since the spin and orbital state of the Mn^{3+} barely changes even with applied magnetic field in this configuration.

This mechanism of magnetocapacitance also works for the cell-doubled phase ($T < T_2 = 33$ K), in which the Mn^{3+} spins take almost a coplanar spin structure.[11] In the incommensurate phase ($T_2 = 33$ K $< T < T_1 = 39$ K), on the other hand, the dielectric constant gradually increases with H (Fig. 4), though M exhibits a sharp increase in the low H region [Fig. 2(e)]. One possible scenario to explain this discrepancy is that Mn^{3+} spins take a conical spin structure in the incommensurate phase. In this case, even if magnetic field is applied along the [100] direction so that the cone axis is oriented along the [100] direction and finite magnetization appears in that direction, each spin does not lie within the same plane, as shown in Fig. 1(d). Thus, unlike in the Yafet–Kittel phase or the cell-doubled phase with coplanar spin structures, not only the x^2 but also the y^2 orbital is hybridized with the z^2 state, resulting in the smaller anisotropy of the force constant in the low H region.

For the incommensurate phase ($T_2 < T < T_1$), two types of magnetic structures have been proposed. One is a sinusoidal spin structure proposed by Chardon et al.,[12] where the Mn^{3+} spins are modulated sinusoidally but keep a coplanar structure. The other is a conical spin structure proposed by Jensen et al.,[11] where half of the Mn^{3+} spins ("conical spin") take the conical spin structure with the cone axis along the [110] direction and the propagation vector (q) along the [10±1] direction, but the other half spins ("coplanar spin") lie on the (1–10) plane. Our model of magnetocapacitance indicates that the conical model is more likely in the incommensurate phase. Note that the gradual increase in the dielectric constant with the applied magnetic field in this phase suggests a continuous change of the Mn^{3+} spin structure from the conical to the coplanar one with the applied magnetic field. It should be also noted that, according to the inverse Dzyaloshinskii-Moriya mechanism, local electric polarization is induced between the conical and the neighboring coplanar spins. However, the local electric polarization is cancelled out for the neighboring pairs in this magnetic structure, and thus macroscopic electric polarization is not produced in the incommensurate phase, consistent with the present experimental result.

It should be pointed out that this mechanism of the coupling between dielectric properties and magnetism is applicable not only to Mn_3O_4 but also to other systems with the orbital degree of freedom and spin-orbit coupling, such as $Tb_3Fe_5O_{12}$.[14]

In conclusion, we measured the dielectric constant and strain of Mn_3O_4 with applied magnetic field. We found that the dielectric constant has clear anomalies at the magnetic phase transition temperatures. We also found that the in-plane dielectric constant exhibits a large anisotropic magnetocapacitance, whose behavior against magnetic field strongly depends on the magnetic structure. These results can be explained by the change of the orbital state of the Mn^{3+} ion due to the inverse process of single-ion spin anisotropy.

[1] Y. Yamasaki, S. Miyasaka, Y. Kaneko, J.-P. He, T. Arima, and Y. Tokura, Phys. Rev. Lett. **96**, 207204 (2006).

[2] Hosho Katsura, Naoto Nagaosa, and Alexander V. Balatsky, Phys. Rev. Lett. **95**, 057205 (2005).

[3] M. Mostovoy, Phys. Rev. Lett. **96**, 067601 (2006).

[4] T. Suzuki, M. Katsumura, K. Taniguchi, T. Arima, and T. Katsufuji, Phys. Rev. Lett. **98**, 127203 (2007).

[5] H. Takei, T. Suzuki, and T. Katsufuji, Appl. Phys. Lett. **91**, 072506 (2007).

[6] K. I. Kugel, and D. I. Khomskii, Zh. Eksp. Teor. Fiz. **64**, 369 (1973) [Sov. Phys. JETP **37**, 725 (1973)].

[7] H. Tsunetsugu and Y. Motome, Phys. Rev. B **68**, 060405(R) (2003).

[8] T. Suzuki, K. Adachi, and T. Katsufuji, J. Phys.: Conf. Ser. **31**, 235 (2006).

[9] R. Tackett, G. Lawes, B. C. Melot, M. Grossman, E. S. Toberer, and R. Seshadri, Phys. Rev. B **76**, 024409 (2007).

[10] J. B. Goodenough and A. L. Loeb, Phys. Rev. **98**, 391 (1955).

[11] G. B. Jensen and O. V. Nielsen, J. Phys. C **7**, 409 (1974).

[12] B. Chardon and F. Vigneron, J. Magn. Magn. Mater. **58**, 128 (1986).

[13] J.-H. Chung, J.-H. Kim, S.-H. Lee, T. J. Sato, T. Suzuki, M. Katsumura, and T. Katsufuji, Phys. Rev. B **77**, 054412 (2008).

[14] N. Hur, S. Park, S. Guha, A. Borissov, V. Kiryukhin, and S.-W. Cheong, Appl. Phys. Lett. **87**, 042901 (2005).

[15] T. Katsufuji and H. Takagi, Phys. Rev. B **64**, 054415 (2001).

[16] T. Kimura, S. Kawamoto, I. Yamada, M. Azuma, M. Takano, and Y. Tokura, Phys. Rev. B **67**, 180401(R) (2003).

[17] M. H. L. Pryce, Proc. Phys. Soc., London, Sect. A **63**, 25 (1950).